Chem

CellPress

Article Type

Hierarchical self-assembly of halogen-bonded block copolymer complexes into upright cylindrical domains

Roberto Milani,[1] Nikolay Houbenov,[2] Francisco Fernandez-Palacio,[3] Gabriella Cavallo,[3] Alessandro Luzio,[4] Johannes Haataja,[2] Gabriele Giancane,[5] Marco Saccone,[6] Arri Priimagi,[6] Pierangelo Metrangolo,[1-4,*] Olli Ikkala[2,*]

[1] VTT Technical Research Centre of Finland Ltd, FI-02044 VTT, Espoo, Finland.
[2] HYBER Centre of Excellence, Department of Applied Physics, Aalto University, FI-02150 Espoo, Finland.
[3] Laboratory of Nanostructured Fluorinated Materials (NFMLab), Department of Chemistry, Materials, and Chemical Engineering "Giulio Natta", Politecnico di Milano, I-20131 Milano, Italy.
[4] Center for Nano Science and Technology@PoliMi, Istituto Italiano di Tecnologia, I-20131 Milano, Italy.
[5] Dipartimento Beni Culturali, Università del Salento, I-73100 Lecce, Italy.
[6] Department of Chemistry and Bioengineering, Tampere University of Technology, FI-33101 Tampere, Finland.
* Correspondence: pierangelo.metrangolo@polimi.it (lead contact); olli.ikkala@aalto.fi

SUMMARY

Self-assembly of block copolymers into well-defined, ordered arrangements of chemically distinct domains is a reliable strategy to prepare tailored nanostructures. Microphase separation results from the system minimizing repulsive interactions between dissimilar blocks and maximizing attractive interactions between similar blocks. This separation has also been achieved with supramolecular methods by introducing small-molecule additives binding specifically to one block by noncovalent interactions. Herein, we use halogen bonding as a supramolecular tool which directs the hierarchical self-assembly of low-molecular-weight perfluorinated molecules and diblock copolymers. Microphase separation results into lamellar-within-cylindrical arrangement and promotes upright cylindrical alignment in films upon rapid casting and without further annealing. Such cylindrical domains with internal lamellar self-assemblies can be cleaved by solvent treatment of bulk films resulting into separated and segmented cylindrical micelles, stabilized by halogen-bond based supramolecular crosslinks. These features, alongside the reversible nature of halogen bonding, provide a robust modular approach for nanofabrication.

The Bigger Picture

Directed self-assembly (DSA) is probably the most promising strategy for high-volume cost-effective manufacturing at the nanoscale to support the ever growing needs of the semiconductors market. DSA exploits the spontaneous self-assembly of block copolymers onto lithographically nanopatterned surfaces, resulting into large area fabrication of periodic nanostructures at the scale of a few tens of nanometers. Tailoring block copolymer's structure, periodicity, and orientation is crucial and requires control over features such as block volume fraction, immiscibility, and surface energy. We introduce here an approach based on the use of fluorocarbon additives that specifically form halogen bonds with only one of the blocks. Our approach promotes microphase separation even upon rapid casting and without subsequent solvent annealing, which, along with the reversible nature of the halogen bond, may pave the way to new self-assembly routes towards the alignment and periodicity of block copolymers and nanostructures.

INTRODUCTION

Block copolymers (BCPs) can self-assemble in a series of well-defined, ordered arrangements of the chemically distinct domains providing with a reliable strategy towards

the preparation of tailored nanostructures. This strategy is widely exploited in the semiconductor industry with Directed Self-Assembly (DSA) techniques, which combine self-assembling materials and lithographic nanopatterning to achieve large-area manufacturing of periodic nanostructures at the scale of a few tens of nanometers. Microphase separation arises from the immiscibility of dissimilar blocks, which try to minimize repulsive interactions. Immiscibility of the blocks may be promoted with supramolecular methods by the block-specific complexation of low-molecular-weight additives.[1-7] Therein, a wide variety of additives can be chosen, ranging from amphiphilic molecules to mesogens incorporating chemical groups that mediate supramolecular interactions with polymer chains. Several kinds of noncovalent interactions are useful to bind these additives to polymers, such as ionic interactions, metal coordination, hydrogen bonding, or their combinations.[8-12] However, to the best of our knowledge, there are no examples, to date, using halogen bonding.

On the other hand, halogen bonding has only recently been developed as a supramolecular tool in the design of functional materials.[13] Halogen bond occurs as a net attractive interaction between an electrophilic region associated with a halogen atom in a molecular entity and a nucleophilic region in another, or the same, molecular entity.[14] In spite of their many similarities, halogen and hydrogen bonds differ mainly in aspects such as directionality, hydrophilicity of the involved functional groups, and robustness in various solvent environments. Despite its established role in small-molecule self-assembly,[15,16] halogen bonding has seldom been applied to directing polymer self-assemblies. Examples include molecularly imprinted polymers,[17] liquid crystalline supramolecular polymers,[18] layer-by-layer assemblies,[19] light-responsive polymers,[20] and long-range alignment of polymer self-assemblies.[21] Solution-phase self-assembly of complementary halogen bonding polymers has been reported only recently.[22]

Here we show that halogen bonding directs the supramolecular binding of low-molecular-weight additives to block copolymers to form hierarchical self-assemblies in bulk samples and films, and allows a route to complex micellar nanostructures. In particular, a perfluorinated halogen-bond donor selectively binds its iodines to pyridine nitrogens of poly(4-vinyl pyridine) block copolymer and promotes microphase separation even upon rapid casting and without subsequent annealing, thus indicating the robustness of the approach. This occurs thanks to the tendency of perfluorocarbons to segregate into separate phases,[21,23] which increases the immiscibility of the two polymer blocks described by the Flory-Huggins χ-parameter. High-χ block copolymers are important to prepare assemblies with low periodicity, useful in nanolithography.[24] In films, selective incorporation of perfluorinated compounds allows to control microdomain alignment in upright cylinders by tuning interfacial energies.

Some of us previously reported that 1,8-diiodoperfluorooctane (DIPFO) halogen bonds to low-molecular-weight poly(4-vinylpyridine) (P_4VP) in a 1:2 molar ratio, pairing all iodine atoms with nitrogens.[25] In the present work, poly(styrene)-*block*-poly(4-vinylpyridine) diblock copolymer (PS-*b*-P_4VP; Figure 1) with M_n = 41.3 kDa (PS) and 8.2 kDa (P_4VP) was selected to form microphase-separated P_4VP(DIPFO) complexes with a lamellae-*within*-cylinder structure. Cylindrical structures are particularly interesting for nanolithography and membranes.[2,26,27] The ditopic additive, *i.e.*, DIPFO, was chosen in order to provide supramolecular crosslinking by simultaneous involvement of the two halogen-bond donor sites at either end of the DIPFO.

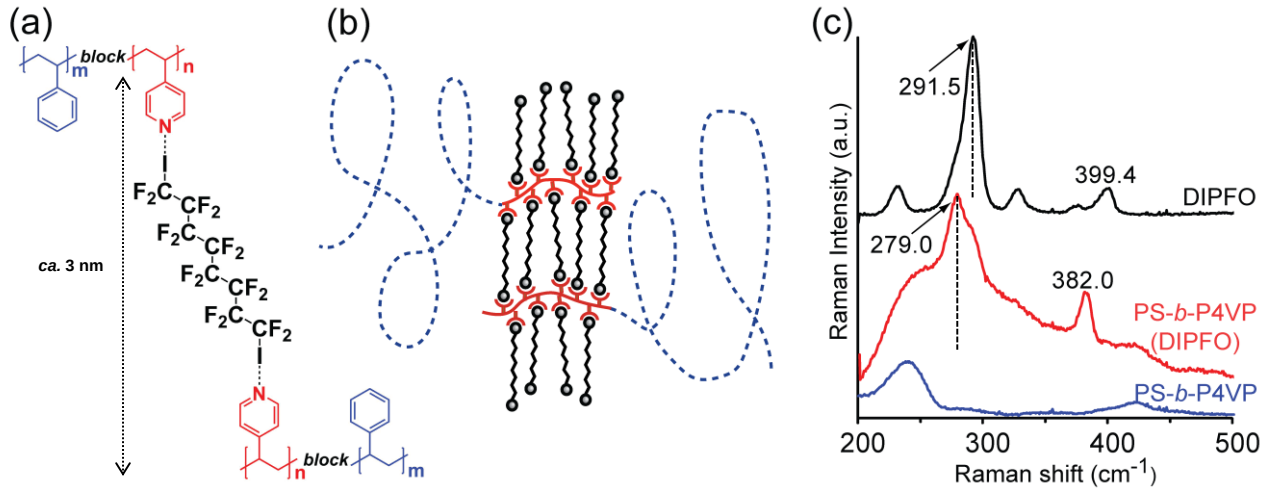

Figure 1.

RESULTS

Sub-millimetric bulk samples

PS-*b*-P4VP(DIPFO) supramolecular assemblies were obtained by mixing PS-*b*-P4VP with DIPFO in a 1:1 I/N atomic ratio (corresponding to overall DIPFO weight fraction of *ca.* 34%) in chloroform and evaporating the solvent in open air until dryness. Binding through halogen bonding was demonstrated by the typical red-shift of the C–I stretching band in the Raman spectrum, from 291.5 cm^{-1} in pure DIPFO to 279.0 cm^{-1} in the complex (Figure 1c), and by several shifts in the 1000-1250 cm^{-1} region of the FTIR spectrum, where C–F stretching vibrations are located (Figure S1). [28] The TGA thermogram of the complex demonstrated the full complexation of the DIPFO, since no significant weight loss was observed between 40 °C and 85 °C (Figure S2). Instead, a 34% weight-loss occurred between 90 °C and 190 °C, indicating that the DIPFO was quantitatively bound to the polymer.

The complexation between PS-*b*-P4VP and DIPFO was also obtained *via* a solvent-free process, *i.e.*, by grinding the two components in a ball mill, reaching a maximum pyridine complexation of about 75% after 4h of milling using a 1:1 I/N atomic ratio, as demonstrated by TGA and IR (Figure S3 and Table S1).

In order to investigate the structure of the PS-*b*-P4VP(DIPFO) supramolecular complex, sub-millimetre thick samples were first prepared from chloroform by drop casting in air, without any annealing. Small-angle X-ray scattering (SAXS) showed that the reflections were distinct but broad. Two closely located peaks were observed at scattering-vector magnitudes of q_2 = 0.016 $Å^{-1}$, plus a partially hidden reflection at q_3 = 0.019 $Å^{-1}$, along with a pronounced higher-order reflection between 0.04 and 0.05 $Å^{-1}$ (Figure 2a). This indicates order at the block copolymer length-scale. A maximum at *ca.* 0.042 $Å^{-1}$ with a tiny shoulder at 0.043 $Å^{-1}$ correspond to the higher-order composite reflections $\sqrt{7}q_2$ and $\sqrt{5}q_3$, suggesting hexagonal and tetragonal packing, respectively. Despite the absence of the expected $\sqrt{3}q_2$ and $\sqrt{2}q_3$ secondary reflections (note the weak scattering between 0.02 $Å^{-1}$ and 0.03 $Å^{-1}$, where reflections are likely screened by the intense main peaks), we suggest a coexistence of regions of hexagonal and tetragonal cylindrical packings at the block copolymer length-scale with spacing between the adjacent P4VP(DIPFO) domains of *ca.* 45 nm (q_2 = 0.016 $Å^{-1}$) and 38 nm (0.019 $Å^{-1}$), respectively. The coexistence of tetragonal and hexagonal phases has been previously reported.[29]

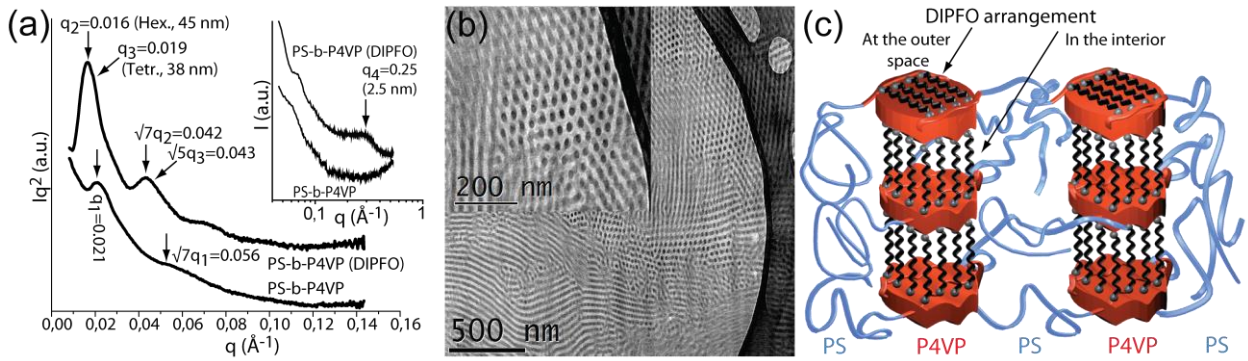

Figure 2.

The structures are further confirmed here by transmission electron microscopy (TEM) on bulk samples and atomic force microscopy (AFM) on films. At the smaller DIPFO length-scale, a broad but pronounced reflection at q_4 = 0.25 Å^{-1} was observed, which indicates structures of *ca.* 2.5 nm periodicity (Figure 2a, inset). This value was not detected for the pure PS-*b*-P4VP (Figure 2a, inset) and is close to the expected spacing of *ca.* 3 nm for two P4VP chains halogen-bonded by a DIPFO molecule (Figure 1a). In fact, the directionality of halogen bonds and the supramolecular crosslinking within the P4VP(DIPFO)-domains caused by the ditopic nature of the DIPFO molecules are expected to cause packing frustration, and the broad peak at q_4 does not come here as a surprise. In conclusion, SAXS supports the hierarchical self-assembly at two-length scale (Figure 2c).

As a reference, pure PS-*b*-P4VP showed in bulk only a main broad reflection at q_1 = 0.021 Å^{-1} and a secondary weak reflection at *ca.* 0.056 Å^{-1} with a ratio of 1:√7, indicating poor hexagonal local order and a cylinder spacing of *ca.* 34 nm. Therefore, upon halogen bonding the DIPFO, the order in bulk improved significantly.

For TEM, a sub-millimetre thick sample of the complex PS-*b*-P4VP(DIPFO) was prepared using drop casting. The sample was microtomed orthogonally to the sample surface to 50-150 nm sections and imaged by TEM. The images showed cylindrical microphases mostly arranged in a hexagonal pattern, although tetragonal arrangement was also observed (Figure 2b), in agreement with the SAXS analysis. The local inhomogeneous orientation of the cylindrical phases in millimeter-thick bulk samples is rather expected and significantly differs from thin film behavior due to interfacial and chain confinement effects.

Spin-coated films

Films were next explored. Films of PS-*b*-P4VP(DIPFO) complex with *ca.* 1 μm thickness were prepared by spin-coating on glass substrates from chloroform. AFM showed self-assembled regions of hexagonal P4VP(DIPFO) patterns with an average diameter of 27.2 ± 5.7 nm and an average center-to-center distance of 45.3 ± 5.8 nm, as well as regions with tetragonal order with center-to-center distance of 39.7 ± 2.8 nm (see Figure 3b). Therefore, the patterns and dimensions in films agree well with those observed in thick samples by SAXS and TEM, giving the first evidence that the patterns in films consist of cylinders that are upright aligned. No clear structuring occurred for pure PS-*b*-P4VP in films prepared similarly (Figure 3a), as also shown by the profile section and the very small root-mean-square roughness (R_{RMS}) of 0.2 nm, when compared with the feature height of about 4 nm and the increased R_{RMS} of 1.2 nm found in PS-*b*-P4VP(DIPFO) films (Figure 3b, Figure S4, and Figure S5).

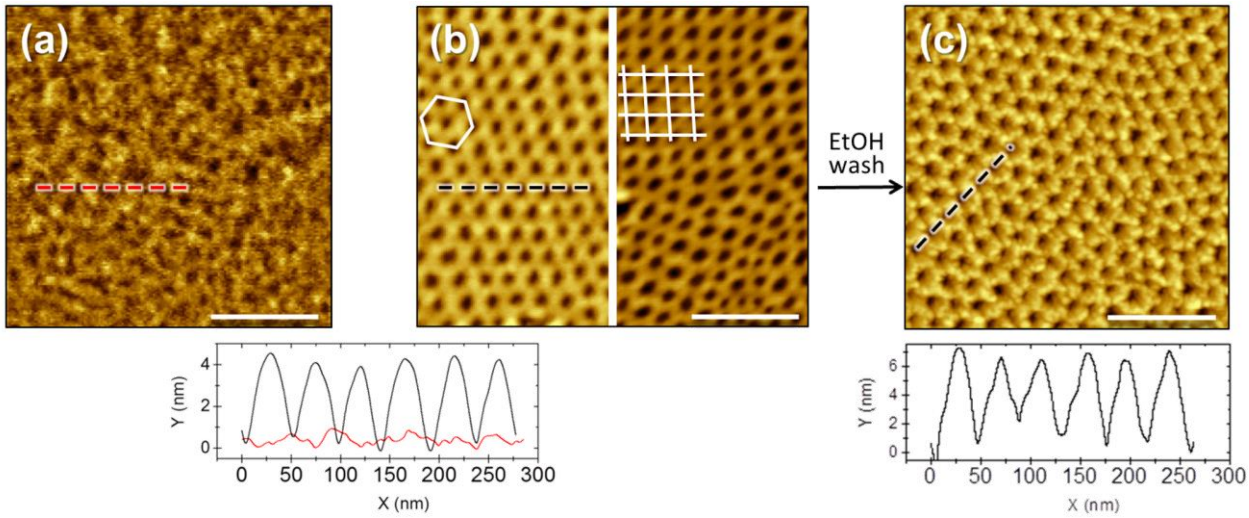

Figure 3.

Further evidence that the patterns observed in films are not spherical domains but upright cylinders was obtained by studying the removal of DIPFO from the PS-*b*-P4VP(DIPFO) films by solvent treatment. Upon washing with ethanol the film retained its periodic structure (Figure 3c and Figure S4), with P4VP residing in the cylinders and surrounded by the intact PS matrix. On the other hand, ethanol displaced DIPFO through the formation of hydrogen bonds with the pyridine nitrogens, and allowed its complete removal as evident by the loss of its FTIR absorption bands (Figure 4). This suggests that there has to be a phase continuity of the P4VP(DIPFO) domains throughout the film, as ethanol does not swell PS, and DIPFO and PS are immiscible.[30] Furthermore, this confirms that the patterns in the films are upright cylinders. The surface top-layer feature height in AFM (*ca.* 6 nm) and the overall roughness of the surface (R_{RMS} = 1.5 nm) were slightly increased, as would be expected upon extraction of DIPFO.[31] Finally, an ethanol-washed film was exposed to gold vapors and the PS-*b*-P4VP polymer template was subsequently extracted in acetone. This allowed deposition of gold nanostructures on the underlying glass substrate with heights typically ranging 3-9 nm (Figure S6).

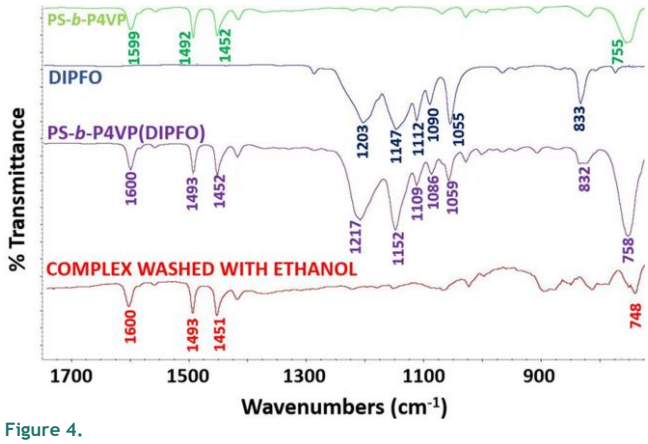

Figure 4.

DISCUSSION

The specific binding of DIPFO by PS-*b*-P4VP thus enhanced the microphase separation tendency and ordering in bulk and in films. In the latter case, upright alignment of the cylindrical microdomains was obtained in a robust way. To achieve upright cylindrical alignment typically requires subtle solvent treatment, surface functionalization, or application of external stimuli, as reviewed recently.[32] Two main factors affect the observed

structure formation in the reported system. First, halogen bonding of DIPFO promotes the self-assembly by effectively and modularly increasing the Flory-Huggins parameter χ, as a result of the omniphobicity of perfluorocarbons and their ensuing tendency towards segregation.[21,23] On the other hand, we used ditopic DIPFO ligands with halogen-bond donor sites at either end to ascertain reliable binding within the P4VP blocks and suppress the excessive volatility of fluorocarbons. This leads to a nanoconfined supramolecular crosslinking of the P4VP chains within the P4VP(DIPFO) microdomains.

Importantly, we suggest that the upright alignment of the P4VP(DIPFO) cylinders in films is promoted by the very low surface energy of DIPFO, *i.e.*, 20.9 dyne/cm[33] (see Figure 2c for its suggested arrangement on the outer surface of the cylinders). This can be compared to a method for upright alignment by using poly(styrene)-*block*-poly(2-vinylpyridine) (PS-*b*-P2VP) with trioctylphosphine (TOPO)-decorated nanoparticles confined in the P2VP-containing cylinders, where the octyl chains of TOPO reduced the air-interface energy of the P2VP-TOPO cylinders.[34]

Finally, we demonstrate the robustness of the ditopic halogen bonding of DIPFO to physically crosslink (see Figure 1) the smaller length scale P4VP nanodomains within P4VP(DIPFO) cylinders to stabilize nanostructures. As toluene is a selective solvent for PS and a poor solvent for P4VP(DIPFO), we aimed to disassemble the larger block copolymer length scale structure and preserve only the P4VP(DIPFO) cylinders incorporating their internal smaller length scale lamellar structure. For that purpose, a bulk sample of PS-*b*-P4VP(DIPFO) was immersed in toluene. After evaporation of the solvent, AFM (Figure 5a, Figure S7) indeed reveals a disordered set of nanofibrils of micrometer length and uniform diameter, fully consistent with those of P4VP(DIPFO) cylinders within the original PS-*b*-P4VP(DIPFO) self-assemblies. This suggests that the fibrillar nanostructures consist of cores that are composed of alternating nanoconfined lamellae of P4VP and DIPFO connected by DIPFO-mediated halogen bonds, the corona consisting of PS-brushes (Figure 5b). As a result, segmented cylindrical micelles are obtained, as visualized in the dried state. Complex cylindrical micelles with patterned cores have previously been achieved from block copolymer solutions by solvent mixtures and solvent exchanges.[35-39] By contrast, the present concept leads to segmented cylindrical micelles from larger scale self-assemblies by solvent induced cleavage. The resulting objects, which are stabilized by halogen bonded supramolecular crosslinks, are relatively rod-like, probably due to the lateral packing of the rod-like DIPFO-molecules.

It is worth noting to point out that the formation of these structures is exclusively favored by the hydrophobic nature of halogen bonding, which allows easy processing of ditopic additives like DIPFO in relatively low polarity solvents such as chloroform. This would be clearly more difficult or impossible to accomplish with related ditopic hydrogen-bond donors, relying, for example, on highly polar moieties such as carboxylic groups,[40] which are clearly not soluble in apolar solvents.

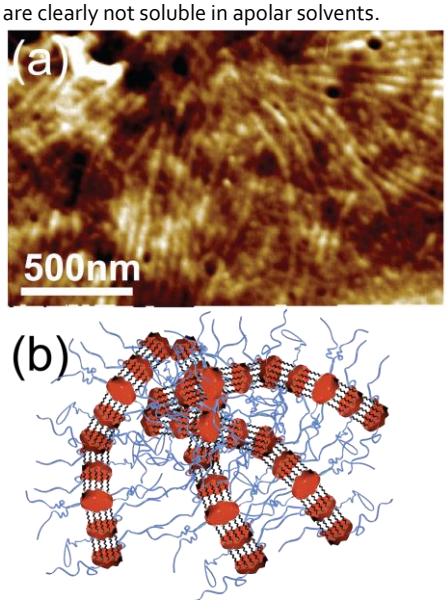

Figure 5.

In conclusion, we have shown that the specific halogen bonding of low-molecular-weight perfluorocarbons to one block of a diblock copolymer directs hierarchical self-assemblies both in bulk and films and allows a route to complex micelles. As a model system we used ditopic, rod-like DIPFO molecules to form halogen bonds at either end with the pyridines of PS-*b*-P4VP, which leads to cylindrical self-assemblies at the block copolymer length-scale and to nanoconfined lamellar halogen-bonded supramolecular networks within the P4VP(DIPFO) cylinders. This demonstrates that halogen bonding can be used to direct block copolymer self-assembly into nanostructured films and complex polymeric nanostructures. In particular, the design choice of a small fluorocarbon molecule as halogen-bond donor allows for the synergistic use of this noncovalent interaction together with surface energy reduction effects, ultimately providing a robust pathway to upright cylindrical arrangement even in relatively thick films. Importantly, significant film nanostructuring is obtained without any need of further thermal or solvent-based annealing. Furthermore, the more hydrophobic nature of halogen bonding in comparison with hydrogen bonding allows for the use of ditopic additives in low polarity solvents, which are often not compatible with multifunctional, highly polar hydrogen bonding additives. This advantage can thus provide higher processing flexibility in the preparation of block copolymer films, for example when relatively high volume fractions of non-polar polymer blocks are involved. As block copolymers with different compositions can be selected for diverse self-assemblies, we foresee that our approach may be of general interest to modularly increase the effective repulsion (the χ-parameter) between copolymer blocks in bulk and in films, and to obtain perpendicularly aligned self-assemblies in films, and complex nanostructures in facile way.

EXPERIMENTAL PROCEDURES

Solid state synthesis of the complex

Solid-state synthesis of the complex between PS-*b*-P4VP and DIPFO was performed by using a Retsch MM 400 ball mill with 5.0 mL stainless steel vessels, operating at 30 Hz. PS-*b*-P4VP and DIPFO were mixed in either 1:2 DIPFO:vinylpyridine molar ratio (N/I atomic ratio 1:1; 33 wt% DIPFO) or 1:4 DIPFO:vinylpyridine molar ratio (N/I atomic ratio 2 :1; 17 wt% DIPFO) for durations varying from 2 to 8 hours.

Preparation of complex bulk samples from solution

PS-*b*-P4VP and DIPFO were dissolved in $CHCl_3$ separately at 0.1 $g.mL^{-1}$ concentration. The PS-*b*-P4VP solution was added dropwise to the DIPFO solution while sonicating in an ultrasonic bath, in order to reach a final 1:2 DIPFO:vinylpyridine molar ratio.
Thick films were prepared by drop-casting on glass slides and allowing the solvent to evaporate at room conditions.

Preparation of complex films from solution and removal of the DIPFO by washing

Thin films of the complex were prepared by spin-coating on silicon and glass slides at 500 rpm. The removal of DIPFO was performed by placing the films overnight in ethanol. The thicknesses of the films were measured with a KLA Tencor Alpha-Step Surface Profiler.

Metalation experiments

Ethanol washed complex films as above were coated with a 5 nm thick gold layer through Physical Vacuum Deposition (PVD) using a MB-ProVap-3 glove-box workstation (Tungsten source). Evaporation was carried out at a pressure of 5×10^{-6} mbar with a constant rate of 0.2-0.3 Å/sec.

Cleaving P4VP(DIPFO) cylinders for segmented cylindrical micelles

A bulk sample of PS-*b*-P4VP(DIPFO) was immersed in toluene (1 mg of PS-*b*-P4VP(DIPFO) in 1 mL toluene overnight), and subsequently diluted by a factor of 10 with additional toluene. The resulting nanostructures were studied using AFM after evaporation of toluene.

SUPPLEMENTAL INFORMATION

Supplemental Information includes the description of used materials, instrumentation and full characterization procedures, as well as seven supplemental figures and one table.

AUTHOR CONTRIBUTIONS

Conceptualization, P.M. and O.I; Methodology, P.M., O.I., R.M., and N.H.; Investigation, F.F.-P., N.H., G.C., A.L., J.H., G.G., and M.S.; Writing – Original Draft, R.M. and N.H.; Writing – Review and Editing, P.M., O.I., R.M., N.H., F.F.-P., G.C., A.L. and A.P.; Funding Acquisition, P.M. and O.I.; Supervision, P.M., O.I. and R.M.

ACKNOWLEDGMENTS

This work was carried out under the Academy of Finland's Centres of Excellence Programme (2014-2019) and made use of the Aalto University Nanomicroscopy Center (Aalto-NMC) premises. The European Research Council (ERC) is gratefully acknowledged for funding the Starting Grant FOLDHALO (Grant Agreement Number 307108) to P. M. and the Advanced Grant MIMEFUN to O. I. This work was also partially supported by the Academy of Finland under the projects no.s 260565, 276537, and 284508. Matti Lehtimäki is acknowledged for his XRD support.

REFERENCES AND NOTES

Morris, M. A. (2015). Directed Self-Assembly of Block Copolymers for Nanocircuitry Fabrication. Microelectron. Eng. *132*, 207–217.

1. Ikkala, O., and ten Brinke, G. (2002). Functional Materials Based on Self-Assembly of Polymeric Supramolecules. Science *295*, 2407–2409.
2. Sidorenko, A., Tokarev, I., Minko, S., and Stamm, M. (2003). Ordered Reactive Nanomembranes / Nanotemplates from Thin Films of Block Copolymer Supramolecular Assembly. J. Am. Chem. Soc. *125*, 12211–12216.
3. Houbenov, N., Haataja, J. S., Iatrou, H., Hadjichristidis, N., Ruokolainen, J., Faul, C. F. J., and Ikkala, O. (2011). Self-Assembled Polymeric Supramolecular Frameworks. Angew. Chem., Int. Ed. *50*, 2516–2520.
4. Zhao, Y., Thorkelsson, K., Mastroianni, A. J., Schilling, T., Luther, J. M., Rancatore, B. J., Matsunaga, K., Jinnai, H., Wu, Y., Poulsen, D., et al. (2009). Small-molecule-directed nanoparticle assembly towards stimuli-responsive nanocomposites. Nat. Mater. *8*, 979–985.
5. Tung, S., Kalarickal, N. C., Mays, J. W., and Xu, T. (2008). Hierarchical Assemblies of Block-Copolymer-Based Supramolecules in Thin Films. Macromolecules *41*, 6453–6462.
6. Zhu, L., Tran, H., Beyer, F. L., Walck, S. D., Li, X., Ågren, H., Killops, K. L., and Campos, L. M. (2014). Engineering Topochemical Polymerizations Using Block Copolymer Templates. J. Am. Chem. Soc. *136*, 13381–13387.
7. Morris, M. A. (2015). Directed self-assembly of block copolymers for nanocircuitry fabrication. Microelectron. Eng. *132*, 207–217.
8. Hagaman, D., Enright, T. P., and Sidorenko, A. (2012). Block Copolymer Supramolecular Assembly beyond Hydrogen Bonding. Macromolecules *45*, 275–282.
9. Madhavan, P., Peinemann, K., and Nunes, S. P. (2013). Complexation-Tailored Morphology of Asymmetric Block Copolymer Membranes. ACS Appl. Mater. Interfaces *5*, 7152−7159.
10. Valkama, S., Lehtonen, O., Lappalainen, K., Kosonen, H., Castro, P., Repo, T., Torkkeli, M., Serimaa, R., ten Brinke, G., Leskelä, M., et al. (2003). Multicomb Polymeric Supramolecules and Their Self-Organization: Combination of Coordination and Ionic Interactions. Macromol. Rapid Commun. *24*, 556–560.
11. Bigall, N. C., Nandan, B., Gowd, E. B., Horechyy, A., and Eychmüller, A. (2015). High-Resolution Metal Nanopatterning by Means of Switchable Block Copolymer Templates. ACS Appl. Mater. Interfaces *7*, 12559–12569.
12. Roche, C., Sun, H., Prendergast, M. E., Leowanawat, P., Partridge, B. E., Heiney, P. A., Araoka, F., Graf, R., Spiess, H. W., Zeng, X., et al. (2014). Homochiral Columns Constructed by Chiral Self-Sorting During Supramolecular Helical Organization of Hat-Shaped Molecules. J. Am. Chem. Soc. *136*, 7169–7185.
13. Priimagi, A., Cavallo, G., Metrangolo, P., and Resnati, G. (2013). The halogen bond in the design of functional supramolecular materials: recent advances. Acc. Chem. Res. *46*, 2686–2695.
14. Desiraju, G. R., Ho, P. S., Kloo, L., Legon, A. C., Marquardt, R., Metrangolo, P., Politzer, P., Resnati, G., and Rissanen, K. (2013). Definition of the halogen bond (IUPAC Recommendations 2013). Pure Appl. Chem. *85*, 1711–1713.
15. Mukherjee, A., Tothadi, S., and Desiraju, G. R. (2014). Halogen bonds in crystal

engineering: like hydrogen bonds yet different. Acc. Chem. Res. *47*, 2514–2524.
16. Cavallo, G., Metrangolo, P., Milani, R., Pilati, T., Priimägi, A., Resnati, G., and Terraneo, G. (2016). The Halogen Bond. Chem. Rev. *116*, 2478–2601.
17. Takeuchi, T., Minato, Y., Takase, M., and Shinmori, H. (2005). Molecularly imprinted polymers with halogen bonding-based molecular recognition sites. Tetrahedron Lett. *46*, 9025–9027.
18. Xu, J., Liu, X., Lin, T., Huang, J., and He, C. (2005). Synthesis and Self-Assembly of Difunctional Halogen-Bonding Molecules: A New Family of Supramolecular Liquid-Crystalline Polymers. Macromolecules *38*, 3554–3557.
19. Wang, F., Ma, N., Chen, Q., Wang, W., and Wang, L. (2007). Halogen bonding as a new driving force for layer-by-layer assembly. Langmuir *23*, 9540–9542.
20. Saccone, M., Dichiarante, V., Forni, A., Goulet-Hanssens, A., Cavallo, G., Vapaavuori, J., Terraneo, G., Barrett, C. J., Resnati, G., Metrangolo, P., et al. (2015). Supramolecular hierarchy among halogen and hydrogen bond donors in light-induced surface patterning. J. Mater. Chem. C *3*, 759–768.
21. Houbenov, N., Milani, R., Poutanen, M., Haataja, J., Dichiarante, V., Sainio, J., Ruokolainen, J., Resnati, G., Metrangolo, P., and Ikkala, O. (2014). Halogen-bonded mesogens direct polymer self-assemblies up to millimetre length scale. Nat. Commun. *5*, 4043.
22. Vanderkooy, A., and Taylor, M. S. (2015). Solution-phase self-assembly of complementary halogen bonding polymers. J. Am. Chem. Soc. *137*, 5080–5086.
23. Krieg, E., Weissman, H., Shimoni, E., Bar On Ustinov, A., and Rybtchinski, B. (2014). Understanding the effect of fluorocarbons in aqueous supramolecular polymerization: ultrastrong noncovalent binding and cooperativity. J. Am. Chem. Soc. *136*, 9443–9452.
24. Sinturel, C., Bates, F. S., and Hillmyer, M. A. (2015). High χ–Low N Block Polymers: How Far Can We Go? ACS Macro Lett. *4*, 1044–1050.
25. Bertani, R., Metrangolo, P., Moiana, A., Perez, E., Pilati, T., Resnati, G., Rico-Lattes, I., and Sassi, A. (2002). Supramolecular route to fluorinated coatings: Self-assembly between poly(4-vinylpyridines) and haloperfluorocarbons. Adv. Mater. *14*, 1197–1201.
26. Peinemann, K.-V., Abetz, V., and Simon, P. F. W. (2007). Asymmetric superstructure formed in a block copolymer via phase separation. Nat. Mater. *6*, 992–996.
27. Bang, J., Jeong, U., Ryu, D. Y., Russell, T. P., and Hawker, C. J. (2009). Block Copolymer Nanolithography: Translation of Molecular Level Control to Nanoscale Patterns. Adv. Mater. *21*, 4769–4792.
28. Cardillo, P., Corradi, E., Lunghi, A., Meille, V., Messina, M. T., Metrangolo, P., and Resnati, G. (2000). The N···I Intermolecular Interaction as a General Protocol for the Formation of Perfluorocarbon-Hydrocarbon Supramolecular Architectures. Tetrahedron *56*, 5535–5550.
29. Nandan, B., Vyas, M. K., Böhme, M., and Stamm, M. (2010). Composition-dependent morphological transitions and pathways in switching of fine structure in thin films of block copolymer supramolecular assemblies. Macromolecules *43*, 2463–2473.
30. McCarty, L. S., Winkleman, A., and Whitesides, G. M. (2007). Electrostatic self-assembly of polystyrene microspheres by using chemically directed contact electrification. Angew. Chem., Int. Ed. *46*, 206–209.
31. Mäki-Ontto, R., De Moel, K., De Odorico, W., Ruokolainen, J., Stamm, M., Ten Brinke, G., and Ikkala, O. (2001). "Hairy tubes": mesoporous materials containing hollow self-organized cylinders with polymer brushes at the walls. Adv. Mater. *13*, 117–121.
32. Albert, J. N. L., and Epps III, T. H. (2010). Self-assembly of block copolymer thin films. Mater. Today *13*, 24–33.
33. http://www.lookchem.com/1-8-Diiodoperfluorooctane/.
34. Lin, Y., Böker, A., He, J., Sill, K., Xiang, H., Abetz, C., Li, X., Wang, J., Emrick, T., Long, S., et al. (2005). Self-directed self-assembly of nanoparticle/copolymer mixtures. Nature *434*, 55–59.
35. Li, Z., Hillmyer, M.A., and Lodge, T.P. (2006). Laterally Nanostructured Vesicles, Polygonal Bilayer Sheets, and Segmented Wormlike Micelles. Nano Letters *6*, 1245-1249.
36. Wang, X., Guerin, G., Wang, H., Wang, Y., Manners, I., and Winnik, M. A. (2007). Cylindrical Block Copolymer Micelles and Co-Micelles of Controlled Length and Architecture. Science *317*, 644-647.
37. Dupont, J., and Liu, G. (2010). ABC triblock copolymer hamburger-like micelles, segmented cylinders, and Janus particles. Soft Matter *6*, 3654-3661.
38. Gröschel, A. H., Schacher, F. H., Schmalz, H., Borisov, O. V., Zhulina, E. B., Walther, A., and Müller, A. H. E. (2012). Precise hierarchical self-assembly of multicompartment micelles. Nat. Commun. *3*, 710.
39. Qiu, H., Hudson, Z. M., Winnik, M. A., Manners, I. (2015). Multidimensional hierarchical self-assembly of amphiphilic cylindrical block comicelles. Science *347*, 1329-1332.
40. Böhme, M., Kuila, B., Schlörb, H., Nandan, B., Stamm, M. (2010). Thin films of block copolymer supramolecular assemblies: Microphase separation and nanofabrication. Phys. Status Solidi *247*, 2458–2469.

Figure 1. System design and proof of halogen bonding
(a) Molecular design of the target PS-*b*-P4VP(DIPFO) complex.
(b) Supramolecular scheme of the target PS-*b*-P4VP(DIPFO) system.
(c) Raman spectra of pure components and the complex indicating occurrence of halogen bonding manifested in the C-I stretching band red-shift.

Figure 2. Structural characterization of sub-millimeter bulk samples
(a) SAXS patterns of PS-*b*-P4VP and PS-*b*-P4VP(DIPFO) prepared by drop casting.
(b) TEM micrograph of a microtomed PS-*b*-P4VP(DIPFO) bulk sample.
(c) Schematic representation of the observed lamellae-within-cylinder structure of the PS-*b*-P4VP(DIPFO) complex for the used block lengths. The suggested arrangement of DIPFO molecules within the interior illustrate the 2.5 nm periodicity, while the very low surface energy of the perfluorinated compounds is suggested to direct the upright cylindrical alignment at the outer surface of the films.

Figure 3. Structural characterization of spin-coated films
AFM topographic micrographs of films prepared by spin-coating. Profile sections taken along the dashed lines are reported below the images. Scale bars: 200 nm. Large-scale AFM micrographs and analysis of P4VP/DIPFO domain diameter and center-to-center distance are available in the Supplemental Information, Figures S4 and S5.
(a) Pure PS-*b*-P4VP.
(b) Complex PS-b-P4VP(DIPFO), showing the presence of regions with hexagonal and tetragonal order.
(c) PS-*b*-P4VP(DIPFO) film after ethanol washing.

Figure 4. FTIR proof of DIPFO removal
ATR-FTIR spectra of PS-*b*-P4VP, DIPFO, and of a PS-*b*-P4VP(DIPFO) film as prepared and after ethanol washing, showing that DIPFO can be completely removed.

Figure 5. Segmented cylindrical micelles stabilized by halogen bonding
(a) AFM of cylindrical micelles consisting of cores of alternating layers of P4VP and DIPFO, and PS brushes coronas, prepared by cleaving the P4VP(DIPFO) cylinders from the PS-matrix by a PS-selective solvent. See also Figure S7 for larger scale images.
(b) Representative scheme of the segmented cylindrical micelles.